Detection and classification of citrus green mold caused by *Penicillium digitatum* using multispectral imaging

Mahmood Reza Golzarian[a], Narges Ghanei Ghooshkhaneh[b], Mojtaba Mamarabadi[c]

[a] Department of Biosystems Engineering, Ferdowsi University of Mashhad, Iran

E-mail: m.golzarian@um.ac.ir

[b] Department of Biosystems Engineering, Ferdowsi University of Mashhad, Mashhad, Iran

E-mail: na.ghanei@mail.um.ac.ir

[c] Department of Plant protection, Ferdowsi University of Mashhad, Iran

E-mail: mamarabadi@um.ac.ir

Corresponding Author:

Mahmood Reza Golzarian

Department of Biosystems Engineering, Ferdowsi University of Mashhad, P. O. Box 1163, Mashhad, Iran

Tel.: (+ 98) 51 3880 5808

Fax: (+ 98) 51 3880 5808

E-mail: m.golzarian@um.ac.ir

Abstract

BACKGROUND: Fungal decay is a prevalent condition that mainly occurs during transportation of products to consumers (from harvest to consumption) and adversely affect post-harvest operations and sales of citrus fruit. There are a variety of methods to control pathogenic fungi including UV-assisted removal of fruit with suspected infection before storage, which is a time-taking task coupled with human health risks. Therefore, it is essential to adopt efficient dependable alternatives for early decay detection. In this paper

This article has been accepted for publication and undergone full peer review but has not been through the copyediting, typesetting, pagination and proofreading process, which may lead to differences between this version and the Version of Record. Please cite this article as doi: 10.1002/jsfa.8865

detection of orange decay caused by *Penicillium* genus fungi using spectral imaging, a novel automated inspection technique for agricultural products, was examined.

RESULTS: The reflectance parameter (including mean reflectance), and reflectance distribution parameters of surface (including standard deviation and skewness) were extracted from decayed and rotten regions of infected samples and the healthy regions of non-infected samples. The classification accuracy of rotten, decayed and healthy regions at four and five days after fungal inoculation was 98.6 % and 100 % using the mean values and skewness of 500 nm, 800 nm and 900 nm spectra and MNDVI.

CONCLUSION: Comparison results between healthy and infected samples showed that early real-time detection of *Penicillium digitatum* using multispectral imaging was possible within the near infrared (NIR) range.

Keywords: Multispectral imaging, *Penicillium digitatum* fungi, Storage, Real-time detection

Introduction

The orange tree is the highest grown citrus tree by number and its economic life is between 50 to 60 years. Citrus fruit have the largest production (80 million tons year^{-1}) in the world compared to other fruit. This indicates their implications for the world economy.[1] Pathologic diseases and physiological disorders are two of the factors contributing to losses.[2] Pathogenic viruses, fungi and bacteria cause pathologic losses in citrus fruit during harvest, packaging, transportation and storage. One of the most important post-harvest pathologic diseases of citrus fruit is the green mold caused by *Penicillium digitatum* fungus. It spreads through pores and wounds on a number of skin oil glands. If suitable temperature and moisture conditions are available, it creates watery stains on the fruit peel that would further create white mycelia. When stain sizes reach 2.5 cm to 5 cm, the production of olive-green spores begins.[3] The rot gradually spreads, and rottenness covers a major part of or the whole fruit. This rot can be controlled by ensuring suitable conditions with low temperature and moisture content, which can be achieved by using proper warehouse ventilation, removal of fruit with suspected infection, fungicide-drenched fruit wrapping papers, fungicide solution baths for fruit, and sterilizing the warehouse and boxes.[4] UV light can be also used to improve fruit resistance to green decay.[5] Almost all these approaches have been tested for controlling green and blue decay with nearly practical results. However, removal of fruit with suspected infection has not received serious research attention. At same time, UV-assisted removal of suspected fruit before storage, when visual detection is very difficult, is being used in packaging lines in some countries. Since UV light is detrimental to operators, spectral imaging has been shown to be an effective method for quality assessment

of agricultural products and can detect fruit with fungal infection. Peel defects have different spectral reflectance in certain segments of the electromagnetic spectrum,[1] thus spectral imaging has been adopted in the literature to detect and distinguish peel defects of citrus fruit. For example, a study used machine vision systems with lighting within fluorescence and UV spectra in combination with multispectral imaging to detect minor defects (e.g. thrips, scarring and sooty mold) and severe defects (e.g. Anthracnose, stem-end injury and green mold).[6] Hyperspectral imaging as a novel method for non-destructive quality measurement of variety of agricultural products have been used in detecting foreign substance on fresh-cut lettuce,[7] Modelling postharvest quality of blueberry,[8] evaluating of bacteria-infected watermelon seeds[9] and etc. Hyperspectral images (500-800 nm) were also employed to detect thrips in citrus fruit.[10] Different studies have used PCA to select multiple wavelengths that can be potentially used in an online multispectral imaging system. The system was able to detect common defects of oranges with the help of hyperspectral imaging (400-1000 nm) in samples with insect damage, wind scarring, thrips and scale infestation.[11] There is a large body of research on detection of orange green mold using spectrometric and hyperspectral techniques. Blasco[12] used NIR spectroscopy (NIRS) for early detection of *penicillium* rot and *Alternaria citri* in navel oranges. Their results showed that the reflectance spectrum of the infected tissues at 1050 nm was lower than the intact area. This is probably due to the fact that fungal sporulation of fruit peel extracts the intracellular fluid leading to water build-up in the infected tissue and its softening. At the same time, the fluid absorbs the NIR spectrum, reducing the IR-range reflectance in the infected area. Another group of researchers used hyperspectral imaging to detect *penicillium digitatum* molds of mandarin oranges. Various methods (including correlation analysis, and genetic algorithm based on linear discriminant analysis (LDA)) have been studied to select optimal bands. They achieved 91.1 % accuracy with 20 optimal spectral bands within the 400 nm to 1000 nm range.[13] In another study, these authors successfully reduced the number of optimal spectral bands to 10 within the 400 nm to 1000 nm range**.** A better detection accuracy (98 %) was realized using classifiers based on artificial neural network and decision tree. Their proposed wavelengths were near to visible spectrum and also the combined spectral index of (800-550)/(800+550).[14] The attempt to select optimal wavelengths effective in detection of green and blue molds of citrus fruit is still ongoing. In this regard, 10 different feature selection methods (e.g. correlation analysis, Fisher's discriminant analysis, and receiver operating characteristic ROC curve) were compared.[15]

From the literature review, it can be concluded that although green mold detection of oranges using multispectral imaging has been studied, we can reduce the number of bands which would make real-time

work possible. So in this study we consider four spectrum and a spectral index for decay detection using multispectral imaging. A proper multispectral imaging system capable of capturing images from spherical or spheroidal shapes (oranges) should be first developed in order to detect orange green mold by multispectral imaging. The samples should be then inoculated with *P. digitatum* fungi. Finally, imaging should be done from the first possible day until the inoculation is clearly visible to naked eye, and spectral information should be extracted from images for analysis. These steps are fully explained in the following sections.

Materials and Methods

It is highlighted that the object of this study is the early detection of rotten region before the decayed region appeared. To explain the terms rotten and decayed, the stages of fungi growth are expressed as follows: first, *Penicillium digitatum* fungi spreads though pores and wounds on a number of skin oil glands, then it creates watery stains on the fruit peel that would further create white mycelia. When the stain size reaches 2.5 cm to 5 cm in diameter, the production of olive-green spores begins. Given that in this study, a sample was punched and injection was done in the hole and under the skin, the region that was immediately around the hole was considered as the decayed region. As a result of fungal growth, a region immediately around the hole area becomes water soaked. This water soaked region was hardly visible to the naked human eye even 4 days after inoculation; this water soaked region is called “rotten” region. Then after day 4, the decayed region gradually becomes white that is as a result of mycelia growth and after that it becomes green and then it spreads. While the expansion of decayed region, the rotten region also is pushed out and spreads; this means healthy regions of peel becomes rotten, then white and then green.

Sample preparation:

Both commercial varieties (Jaffa and Thompson) were purchased from northern orchards of Iran and were transferred to the Nosology Laboratory of Phytopathology Department of Ferdowsi University of Mashhad. A total of 30 Thompson and 30 Jaffa oranges were selected for fungal inoculation, and 10 samples from each variety were considered as control. Additionally, about 20 samples with minor peel defects from each variety were selected. It was further ensured through laboratory tests that these defects were non-pathogenic during culture and pathogenicity test. The samples were harvest at the time of full maturity (Thompson: TSS 11.86 ^{o}Brix and 3.7 pH; Jaffa: TSS 12.5 ^{o}Brix and 3.48 pH).

Orange inoculation with fugal pathogen suspension:

Healthy and size-wise similar oranges were separated and washed. They were then disinfected in three separate solutions (22.2 g kg^{-1} hypochlorite, sterile distilled water and 55.23 g kg^{-1} ethanol) for 30 min in each, and finally dried on filter papers. A 1 mm wide and 2 mm deep hole was drilled in the mid-section of each orange.[16] A micropipette was used to inject 0.02 mL of fungal spore suspension with a concentration of 10^6 spore mL^{-1} into these holes. Each control sample also received similar treatments however they were injected with 0.02 mL of sterile distilled water. The samples were then transferred to a germinator and were kept at 25 °C.

Imaging samples:

The first signs following fungal inoculation were manifested as a rotten stain with variable diameters between 10 to 35 mm, which was hard to notice with naked eyes.[17] The rottenness formation time can be different in each sample, ranging from four days to latest six days.[16] According to pre-tests performed on some orange samples, until the fourth day of infection, the spectral reflections of the orange surface in the 800 nm and 900 nm bands did not have much difference, that is, the early detection on the third day was not possible. In this study, the imaging sessions were started from 4 d after inoculation and continued until 25 d. During these 25 d, the oranges were kept within the germinator at 25 °C. Images were taken in a sterile environment in order to keep the samples within sterile conditions to continue studying the fungal growth.

Spectral Imaging System:

In spectral imaging of agricultural products with spherical or spheroidal shapes, direct or 45° lighting on subjects would lead to intense reflectance, which in turn is a challenge to extracting useful data from images. Therefore, an aluminum hemisphere was used to create uniform lighting. Moreover, the closed housing of the spectral imaging system prevented ambient light leakage. Since tungsten halogen lamps have a good lighting efficiency within the NIR range of the electromagnetic spectrum[18], a total of 12 lamps (12 V, 50 W, DECOSTAR 51 COOL BLUE) were used for lighting purposes. The sensitivity of a standard CCD is about 900 nm[18], thus a Samsung camera (SCB-2000P) equipped with 1/3" Super HAD CCD II was also used. This CCD uses the interline transfer architecture with high quantum efficiency at both visible and NIR ranges of the electromagnetic spectrum[18].

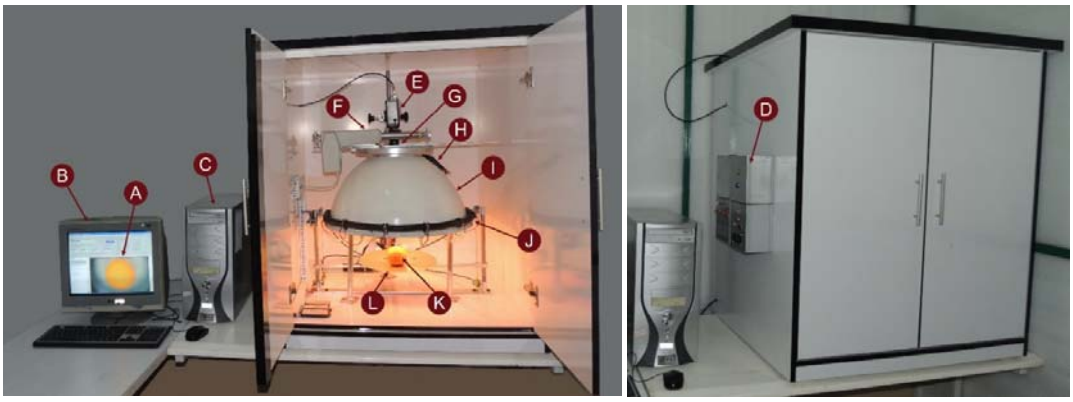

Figure 1. The Vis-NIR spectral imaging system; a. Online image of sample, b. Computer monitor, c. Computer, d. Control panels of lighting system and motors of displacement, e. Vis-NIR camera, f. Guidance system for changing the filters, g. Placement of the filters, h. Cooling fan, i. Aluminum hemisphere of lighting system, j. Light-dispersing illumination system, k. Sample for imaging, l. Plate of sample placement.

Given the resolution of the available Vis-NIR camera (100 nm) and proposed wavelengths of literature review, the selected bands for this study were 500 nm, 700 nm, 800 nm and 900 nm plus the spectral index (800-500)/(800+500) for detection of green mold in oranges, that were close to that proposed wavelengths. Accordingly, a bandpass filter (Thorlabs Crop., USA) was used. In this study, like the NDVI factor, which is a combination of NIR and RED, the spectral index (800-500)/(800+500) was also named as Modified NDVI (MNDVI).

To extract spectral information, the images captured by the multispectral imaging system were used. The effects of lamp lighting variations were removed by calibrating the raw images. To this end, a reference surface with 100 % reflectance was used. In different research studies, barium sulfate[12] and polytetrafluoroethylene (PTFE)[19] were used as reference surfaces. The former was used in this study. Equation (1) was used to obtain the calibrated image.

$$R=\frac{R_{sample}-R_{dark}}{R_{reference}-R_{dark}} \quad (1)$$

Where R is the calibrated image of the sample, R_{sample} is the raw image, $R_{reference}$ is the image of the reference surface, R_{dark} is the image of the reference surface with all lights out[20].

Once images were calibrated, the statistical parameters (such as mean, standard deviation and skewness) were extracted from pixels relating to rotten and decayed parts at different stages (Figure 2). These parameters were computed in MATLAB (v2015, Mathworks Inc, USA). For each region, a mean spectral reflectance value was obtained for 500 nm, 700 nm, 800 nm and 900 nm wavelengths as well as for the spectral index MNDVI. The studied independent variables or factors were orange variety (Jaffa and Thompson), time after inoculation (From here on, the fourth, fifth, seventh, tenth, thirteenth, seventeenth

and twenty fourth day after inoculation are expressed as 4 d, 5 d, 7 d, 10 d, 13 d, 17 d and 24 d, respectively), and region type (healthy, rotten and decayed). The dependent factors were mean reflectance from orange surface at 500 nm, 700 nm, 800 nm and 900 nm spectra. Results were analyzed using a factorial design with a completely randomized layout in SPSS 16 (IBM, USA).

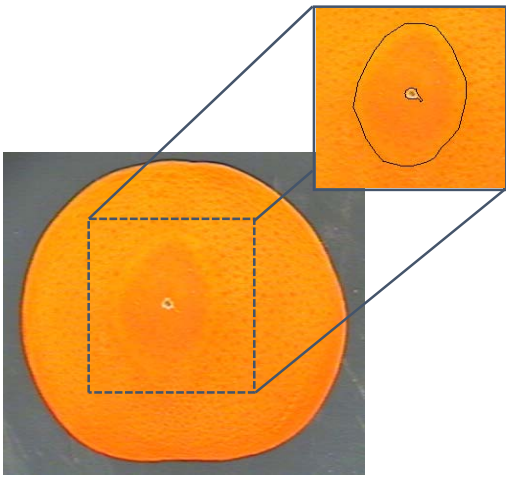

Figure 2. Segmentation method of rotten and decayed parts for feature extraction; these regions become visible to naked eye after about seven days

Results and Discussion

The objective of this study was early detection of infected tissues in oranges, which first manifest as rottenness and turns into decay and spreads over time. Therefore, the infected tissues were divided into rotten and decayed, which were compared to each other. Two orange varieties (Jaffa and Thompson), seven time after inoculation (4 d, 5 d, 7 d, 10 d, 13 d, 17 d and 24 d), and three region types (healthy, rotten that is caused by fruit response to infection, and decayed) were selected, which had effects on orange surfaces reflectance at 500 nm, 700 nm, 800 nm and 900 nm spectra. Accordingly, ANOVA results for each spectrum is shown in Table 1.

Table 1. ANOVA results for the effects of time, variety and region type on spectral reflectance at 500 nm, 700 nm, 800 nm and 900 nm

Source	df	500 nm	700 nm	800 nm	900 nm
time	6	6.099*	10.545*	86.925*	102.846*
variety	1	0.076ns	45.914*	48.799*	138.022*
region type	2	33.181*	899.031*	254.8*	197.900*
time× variety	6	4.298*	1.805ns	0.948ns	4.977*
time× region type	12	8.030*	10.172*	14.613*	10.922*
variety × region type	2	39.187*	40.066*	39.709*	38.358*
time× variety× region type	12	2.307*	1.724ns	1.722ns	1.631ns

* Significant at 5% of probability levels, respectively, ns Non. Significant

ANOVA results showed that the effects of time, region, interaction of time and region, and interaction of variety and region on spectral reflectance at 500 nm and 700 nm spectra were significant ($p < 0.05$) (Table 1). This shows that healthy and infected skin regions of both orange varieties had different reflectance under green and red lights at least at a few times after inoculation. Additionally, the significant effect of orange variety on spectral reflectance at 700 nm showed that surface reflectance values of both orange varieties under nearly red light were different from each other at different times.

ANOVA results showed that the effects of time, orange variety, region, interaction of time and region, and interaction of variety and region on spectral reflectance at 800 nm and 900 nm spectra were significant ($p < 0.05$). In other words, surface reflectance of both orange varieties under NIR light with 800 nm and 900 nm spectral peaks were different from each other at different times.

The statistical analysis was verified by plotting mean reflectance curves at different spectra. In these curves, error bars were drawn based on the 95 % confidence interval (CI). In addition, mean spectral band values were normalized and dimensionless. Figure (3) shows the mean reflectance curve at 500 nm and different times obtained from healthy, decayed and rotten regions of Jaffa and Thompson oranges.

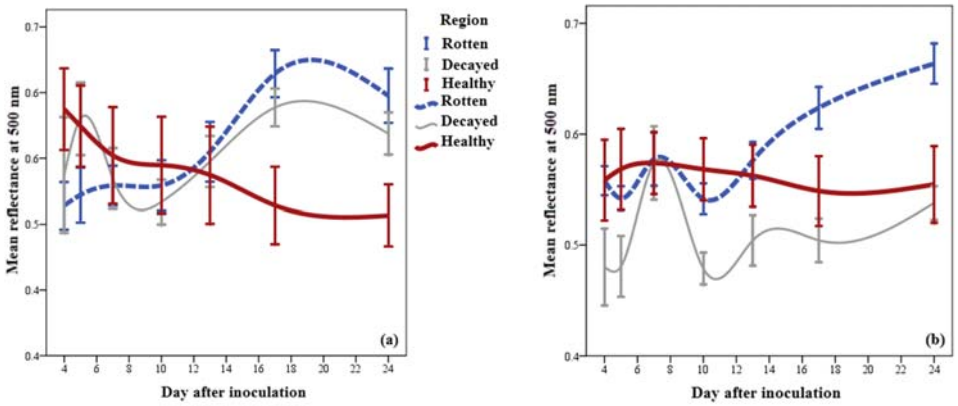

Figure 3. The mean reflectance curve at 500 nm and different times obtained from healthy, decayed and rotten regions; a. Jaffa, and b. Thompson, Error bars: 95 % CI.

According to Figure (3), it can be concluded that, when decay appears, the surface reflectance at 500 nm can be used to detect decayed regions within healthy ones. The purpose of this study was however early detection of infected tissues that first emerge as rottenness, and thus the 500 nm spectrum is not suitable as the rotten and healthy tissues of Jaffa and Thompson oranges can be detected using the 500 nm spectrum only on 17 d and 24 d after the infection.

Reflectance variations of rotten and decayed regions against time can be explained by studying how the rotten region is formed. For instance, the rotten region of Thompson oranges due to its more resistance to fungi was divided into two sub-regions; a sub-region that was infected by fungi and became water soaked (region *a* illustrated in Figure 4) and sub-region that was created as the hypersensitive reaction of cells for preventing fungi growth (region *b* illustrated in Figure 4). This is called "defense region" and it was seen only in Thomson oranges. Accordingly, cells commit suicide to fight with fungi and the dead tissue prevents the spread of fungal pathogens. This phenomenon is called programmed cell death (PCD) or hypersensitive response (HR) caused by fungal pathogen invasion, which is a resistance against pathogens.[21] Observations have revealed that this type of resistance is greater in Thompson than in Jaffa oranges. Additionally, this defense region has a higher reflectance than the rotten region due to its lighter surface. With this background, the large variations in the rotten-region curve of Thompson oranges can be explained with the complementary information of Figure (5). It is be noted that this is a sample of about seven days after inoculation illustrated in figure 4.

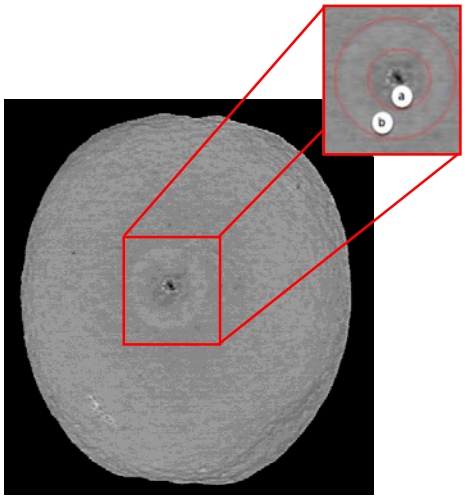

Figure 4. View of the rotten region of Thompson oranges; a. water soaked region, b. defense region

In this study, the rotten region includes the water soaked section around the injection point before emergence of decaying and HR-induced defense rings. In Figure (5a), the point corresponding to it is a result of averaging the reflectance values from the points located at two different regions: fungal-induced rotten (darker) and fruit defense (lighter) regions. In Figure (5b), the fruit defense region has expanded, and thus since it has higher reflectance than the rotten region, its reflectance is also higher than reflectance from section *a*. In section *c* of the image, the defense region has turned into the rotten region with lower reflectance than section *b*. Given the fact that averaging the values of all rotten and decayed points leads to

removal of details and differences between these two regions, and thus affects their accurate detection, it would be better to adopt parameters that reflect variations in surface reflectance (e.g. standard deviation or skewness) to distinguish these regions from each other.

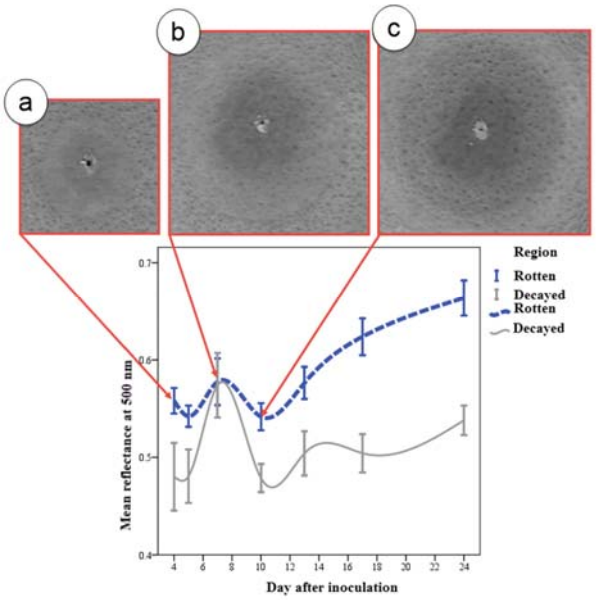

Figure 5. Variations in reflectance of the rotten surface in Thompson oranges at 500 nm and different times, Error bars: 95 % CI.

Figure (6) shows the mean reflectance curve at 700 nm and different times obtained from healthy, decayed and rotten were selected and rotten regions of Jaffa and Thompson oranges. It can be concluded from the curves that 700 nm is not a suitable spectrum for separating rotten and healthy (control) tissues at the early stages of inoculation in Jaffa and Thompson oranges. At the 700 nm spectrum, the decayed region is fully detectable from the healthy region due to lower carotenoid, chlorophyll and flavonoid content that are the effective pigments in absorbing light and in the yellow color of the skin.

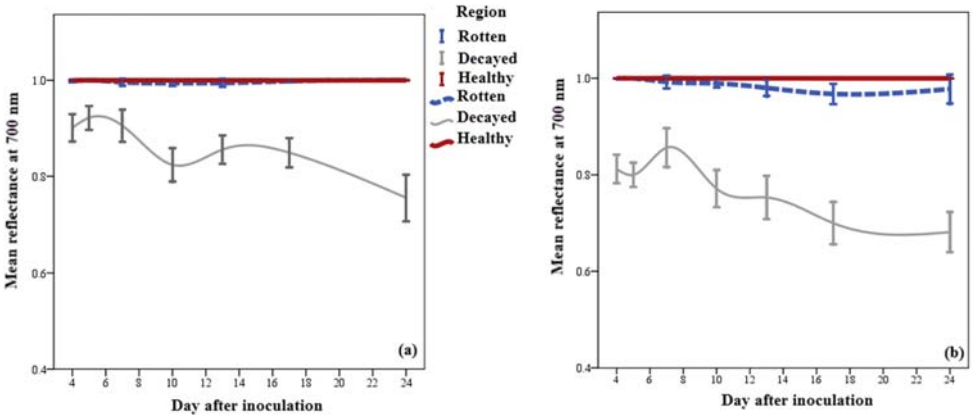

Figure 6. Variations in surface reflectance at different times for healthy, decayed and rotten regions at the 700 nm spectrum; a. Jaffa, and b. Thompson oranges, Error bars: 95 % CI.

Figure (7) shows the curves related to 800 nm and 900 nm spectra and MNDVI of Jaffa oranges. Based on these curves, it is clear that the healthy region can be separated from rotten and decayed regions of Jaffa samples using the 800 nm and 900 nm spectra. These tissues can be also detected by the MNDVI, 13 d after inoculation. Similar results were obtained for Thompson oranges, and thus the 800 nm and 900 nm spectra and the spectral index MNDVI can be used for detection and classification of healthy, rotten and decayed regions. At the 900 nm spectrum, which is the water absorption spectrum, the reflectance of the rotten tissue is lower than that of the intact region because the cell wall is ruptured by fungus and the water is released in the skin. The 800 nm spectrum is also associated with biochemical elements like cellulose and other carbohydrates. The lower reflectance of the rotten surface than the healthy region is due to variations in the internal structure of the epidermis.[17]

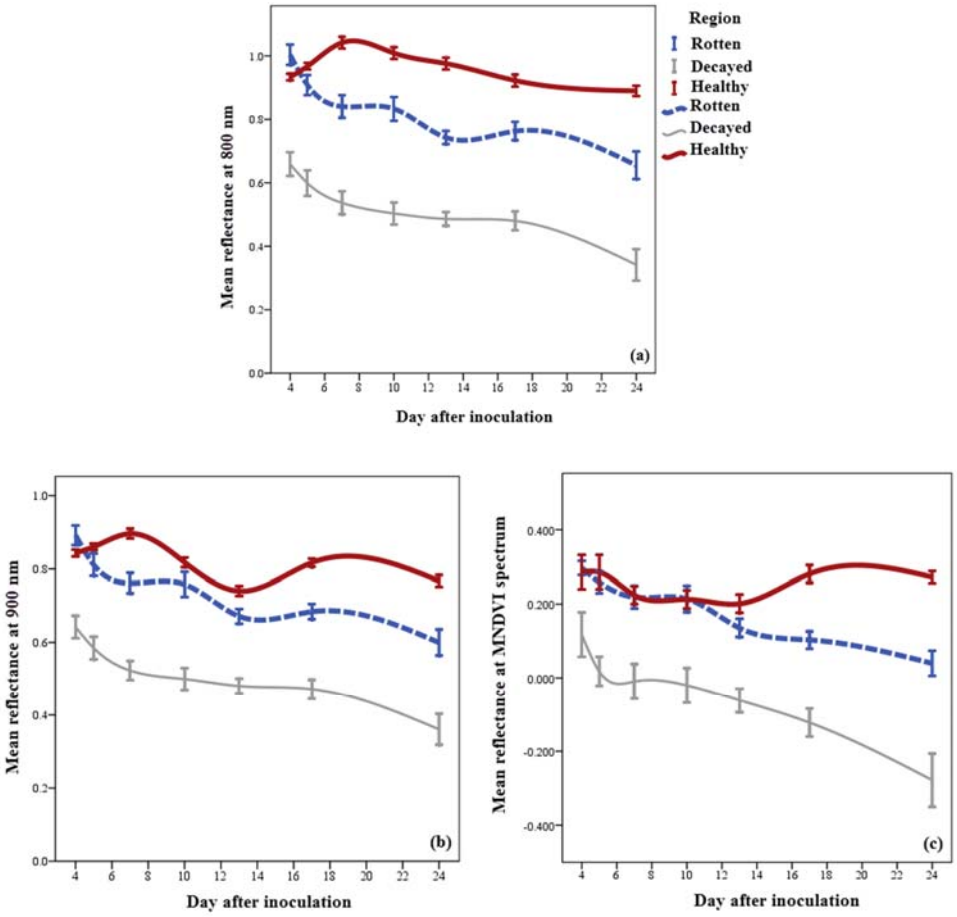

Figure 7. Variations in surface reflectance at different times for healthy, decayed and rotten regions of Jaffa oranges; a. at the 800 nm spectrum, b. at the 900 nm spectrum, and c. at the MNDVI spectrum, Error bars: 95 % CI.

Classification:

Fisher's linear discriminant analysis (LDA) was adopted to classify the different regions on orange surfaces into *healthy* (control), *decayed* and *rotten* based on mean reflectance at 800 nm and 900 nm spectra and the spectral index MNDVI. The classification model was trained and validated using the leave-one-out method. Leave-one-out cross-validation is the special case for k-fold cross-validation where k (the number of folds) is equal to the number of records in the initial dataset. While this can be very useful in some cases, it is probably best saved for datasets with a relatively low number of records. In this method, only one sample is taken out and all other samples are used to build the calibration. By repeating the selection of different samples, the predictions can be made on all samples for the validation procedure. So all samples were used as the training or validation data sets.

Table (2) shows the classification results for separate and combined application of the 800 nm, 900 nm and MNDVI spectra. Since the study aimed at early detection of orange mold, the classification results given in the table belong to the first days after inoculation (4 d, 5 d and 7 d after inoculation).

Table 2. Classification results for healthy, decayed and rotten regions of Jaffa and Thompson oranges at different times and spectra

			Classification accuracy					
Variety	Spectra	Region	4 d	Total	5 d	Total	7 d	Total
Jaffa	800 nm, 900 nm, MNDVI	Rotten	93.3	82.6	89.3	78.8	92.6	96.9
		Decayed	96.7		96.4		100	
		Healthy	10		0.0		100	
	800 nm	Rotten	93.3	81.4	92.9	78.8	92.6	96.9
		Decayed	96.7		92.9		100	
		Healthy	0.0		0.0		100	
	900 nm	Rotten	90.0	80.0	85.7	74.2	88.9	93.8
		Decayed	96.7		89.3		96.3	
		Healthy	0.0		0.0		100	
	MNDVI spectra	Rotten	90.0	75.7	92.2	74.2	92.6	78.1
		Decayed	86.7		82.1		92.6	
		Healthy	10.0		0.0		0.0	
Thompson	800 nm, 900 nm, MNDVI	Rotten	100	92.2	93.1	86.8	92.6	93.8
		Decayed	96.7		93.1		100	
		Healthy	60.0		50.0		80.0	
	800 nm	Rotten	100	92.2	100	85.3	100	90.6
		Decayed	100		93.1		100	
		Healthy	50.0		20.0		40.0	
	900 nm	Rotten	100	97.1	100	74.2	100	84.4
		Decayed	96.7		93.1		100	
		Healthy	90.0		20.0		0.0	

	Rotten	90.0		92.2		92.6	
MNDVI spectra	Decayed	86.7	75.7	82.1	74.2	92.6	78.1
	Healthy	10.0		0.0		0.0	

As shown in Table (2), it can be concluded that, in 4 d after inoculation, the three spectra can be used to detect decayed samples (rotten and decayed regions) of Jaffa and Thompson oranges with high accuracy. However, the accuracy of three spectra for separating healthy samples from rotten ones is high, and these two samples cannot be separated on this day. The three spectra can be used only on 7 d to detect healthy regions of Jaffa and Thompson oranges from rotten and decayed regions with good accuracy. By using the single spectra of 800 nm and 900 nm, the healthy regions of Jaffa oranges is only separatable from rotten and decayed regions only on 7 d, and their classification accuracy for the healthy region is low on other days. Moreover, the MNDVI factor showed no acceptable results for detection of the healthy regions in Jaffa and Thompson samples. At the same time, the spectral band ratio has been used successfully in detection of citrus canker. For example, 95.3 % accuracy using the 730R/830R ratio[22] and 82.9 % using the 687R/630R ratio for test set[23] for detection of citrus canker was achieved. The spectral index MNDVI, as a ratio, was not successful in detection of green mold. This can be due to the damage type as the citrus canker is a time invariable defect classified as a minor damage, whereas the green mold progresses through time and is classified as a severe damage. Moreover, the canker stain color is completely different from the skin color, whereas the green mold emerges as rottenness during its easily stages with a color completely similar to orange skin color, which is undetectable with naked eye. Lorente[24] also introduced the spectral index GREEN NDVI II along with some other visible spectra as a feature group among 74 input features using the characteristic curve of the system performance. They suggested that each feature is necessary for detection of one class (healthy, fungal infection, and minor skin defects).

Different research studies have used LDA for classification purposes. Gomez-Sanchis[13] used two methods (namely, Linear Discriminant Analysis (LDA) and Classification and Regression Tree (CART)) to detect healthy tissues, stem and calyx location, mold and rottenness in mandarin oranges using 20 optimal spectra. Their results showed that non-linear regression tree classification with 95.18 % accuracy outperformed LDA (89.6 %) by only 5.58 %. Baranowski[25] used LDA and reached 90 % accuracy in detection of apple bruised and healthy regions. Kaliramesh[26] also adopted LDA and Quadratic discriminant analysis (QDA) to detect Callosobruchus maculatus in mung bean samples and separate them from healthy ones using hyperspectral images. They used six statistical features (maximum, minimum, mean, median, standard deviation and variance) and ten features of image histogram in optimal spectra for classification purposes.

Their results showed that QDA results (82 % for infected and 89.6 % for healthy tissues) were only 2 % to 6 % higher than LDA results (80.5 % for infected and 83 % for healthy tissues). Literature results showed that LDA is an acceptable classification method. In the previous sections, however, it was shown that averaging all points in rotten and decayed regions leads to removal of details and differences between these points, which in turn affects detection. Therefore, only the parameters that reflect surface reflectance variations should be analyzed. In order to increase the classification accuracy of healthy and infected tissues, parameters like mean, standard deviation and skewness of effective spectra were used.

Table (3) shows classification results using the mean, standard deviation and skewness values of the 500 nm, 800 nm, 900 nm and MNDVI spectra and also the combination of these three values (mean, standard deviation and skewness) of the study spectra for 4 d, 5 d and 7 d for Jaffa oranges. Results showed that use of mean values for these four spectra help clearly detecting rotten and decayed regions on 4 d and 5 d, whereas the healthy tissues were clearly detected only on 7 d. Standard deviation of the study spectra (500 nm, 800 nm, 900 nm and MNDVI) can be used with acceptable accuracy to separate these regions from each other on 5 d and 7 d. This parameter however cannot be adopted to separate the healthy from rotten tissues. Skewness of the study spectra was the only parameter that can be individually used to separate regions. However it showed poor accuracy for detection of rotten from decayed regions on 5 d. Mean and standard deviation values of these spectra can be used to achieve 100 % detection accuracy, with poor results on 4 d and 5 d. Mean and skewness values of the study spectra, and also their mean, standard deviation and skewness values had the highest detection accuracy. Nonetheless, if less computation and shorter time are the goals, mean and skewness values of these spectra are the better option.

Table 3. Classification results for healthy, decayed and rotten regions of Jaffa and Thompson oranges using different combinations of parameters and spectra

		Classification accuracy					
Parameter	Region	4 d	Total	5 d	Total	7 d	Total
Mean of the 500 nm, 800 nm, 900 nm and MNDVI spectra	Rotten	96.7	92.2	92.9	86.4	92.6	96.9
	Decayed	96.7		96.4		100	
	Healthy	70		40.0		100	
Standard deviation of the 500 nm, 800 nm, 900 nm and MNDVI spectra	Rotten	100	82.9	96.3	98.4	100	95.5
	Decayed	93.3		100		89.3	
	Healthy	0.0		100		100	
Skewness of the 500 nm, 800 nm, 900 nm and MNDVI spectra	Rotten	83.3	92.2	78.6	81.8	85.2	90.6
	Decayed	100		78.6		92.6	
	Healthy	100		100		100	
Mean and standard deviation of the 500 nm, 800 nm, 900 nm and MNDVI spectra	Rotten	96.7	95.7	100	98.5	100	100
	Decayed	100		100		100	
	Healthy	80		90		100	
	Rotten	96.7	98.6	92.9	95.5	96.3	98.4

Mean and skewness of the 500 nm, 800 nm, 900 nm and MNDVI spectra	Decayed	100		96.4		100	
	Healthy	100		100		100	
Mean, standard deviation and skewness of the 500 nm, 800 nm, 900 nm and MNDVI spectra	Rotten	100		100		100	
	Decayed	100	100	100	100	100	100
	Healthy	100		100		100	

Table (4) shows classification results using the mean, standard deviation and skewness values of the 500 nm, 800 nm, 900 nm and MNDVI spectra and also the combination of these three values (mean, standard deviation and skewness) of the study spectra for 4 d, 5 d and 7 d for Thompson oranges. According to the results, mean values of the study spectra showed poor results in detection of healthy from rotten tissues. Similar results were observed for standard deviation values. Unlike results for Jaffa oranges, skewness values of the study spectra is not a suitable factor for separating different regions. Again, unlike results for Jaffa oranges, mean and standard deviation values of the study spectra showed poor results in detection of healthy regions on 7 d. Similar to Jaffa oranges, mean and skewness values of the study spectra, and also their mean, standard deviation and skewness values had the highest detection accuracy. Nonetheless, if less computation and shorter time are the goals, mean and standard deviation values of these spectra are sufficiently the better option.

Table 4. Classification results for healthy, decayed and rotten regions of Thompson oranges using different combinations of parameters and spectra

		Classification accuracy					
Parameter	Region	4 d	Total	5 d	Total	7 d	Total
Mean of the 500 nm, 800 nm, 900 nm and MNDVI spectra	Rotten	100		96.6		96.3	
	Decayed	96.7	94.3	100	92.6	100	95.3
	Healthy	70		60.0		80.0	
Standard deviation of the 500 nm, 800 nm, 900 nm and MNDVI spectra	Rotten	100		100		92.6	
	Decayed	100	88.6	100	86.8	100	92.2
	Healthy	20		70.0		70.0	
Skewness of the 500 nm, 800 nm, 900 nm and MNDVI spectra	Rotten	96.7		100		100	
	Decayed	100	97.1	100	98.5	88.9	93.8
	Healthy	90		90.0		90.0	
Mean and standard deviation of the 500 nm, 800 nm, 900 nm and MNDVI spectra	Rotten	100		100		96.3	
	Decayed	100	100	100	98.5	100	95.3
	Healthy	100		90.0		80.0	
Mean and skewness of the 500 nm, 800 nm, 900 nm and MNDVI spectra	Rotten	96.7		100		100	
	Decayed	100	98.6	100	100	100	100
	Healthy	100		100		100	
Mean, standard deviation and skewness of the 500 nm, 800 nm, 900 nm and MNDVI spectra	Rotten	100		100		100	
	Decayed	100	100	100	100	100	100
	Healthy	100		100		100	

Conclusion

The study aimed at early separation of oranges infected with green mold from healthy samples. Samples from two types of oranges (Jaffa and Thompson) were inoculated with *P. digitatum* fungi and were imaged by a multispectral imaging system at different spectra (500 nm, 700 nm, 800 nm and 900 nm) on different days after inoculation (fourth, fifth, seventh, tenth, thirteenth, seventeenth and twenty fourth). Mean reflectance values at 500 nm, 700 nm, 800 nm and 900 nm spectra were extracted. Study results showed that the 500 nm and 700 nm visible spectra are not suitable for early detection of orange green mold using mean reflectance values. At the 700 nm spectrum, it is not possible to separate the infected tissue from the healthy one at the early stages of inoculation in both Jaffa and Thompson oranges. Results indicated that there is a significant difference between the mean reflectance of rotten, decayed and healthy regions in both Jaffa and Thompson samples at the NIR (800 nm and 900 nm) and MNDVI spectral index. Accordingly, the simultaneous use of the 800 nm and 900 nm spectra and the MNDVI spectral index can adopted to classify these regions.

LDA-based classification results showed that mean values of 800 nm and 900 nm spectral bands and the spectral index MNDVI can be used only on 7 d to properly detect rotten, decayed and healthy regions of Jaffa and Thompson oranges. That is, on 4 d and 5 d, the healthy tissue cannot be clearly separated from the rotten region.

The single 800 nm and 900 nm spectra and the spectral index MNDVI were individually sufficient to separate rotten and decayed regions. However, they had low accuracy in detection of healthy regions on a few days.

Mean and skewness, and also standard deviation and skewness of the study spectra had the highest accuracy in detecting Jaffa and Thompson oranges. However, if less computation and shorter time are the goals, mean and skewness values of these spectra are the better option.

In general, it can be concluded that the multispectral imaging method can detect fungus-infected oranges at the early stages.

Acknowledgment

We, the authors, acknowledge Ferdowsi University of Mashhad for providing the funding for doing this research (Grant No. 3/39744). We would also like to thank Dr Nima Khaledi, from the department of Plant Protection, for his laboratory advice and technical assistance during the experiments.

References

1. Moltó E, Blasco J and Gómez-Sanchís J, Analysis of hyperspectral images of citrus fruits, in *Hyperspectral imaging for food quality analysis and control*, ed. by Sun D-W. Academic Press, San Diego, pp. 321-348 (2010).
2. Guleria SPS, Quality assurance for fruits, vegetables and their products, in *Postharvest technology of fruits and vegetables*, ed. by Verma LR and Joshi VK. Induce publishing Co., New Dehli. (2000).
3. Timmer LW, Garnsey SM and Broadbent P, Diseases of citrus, in *Diseases of tropical fruit crops*, ed. by Ploetz RC. CAB International (2003).
4. Ladaniya MS, Postharvest diseases and their management, in *Citrus fruit*. Academic Press, San Diego, pp. 417-XIX (2008).
5. Turtoi M, Ultraviolet light treatment of fresh fruits and vegetables surface: A review. *J Agroaliment Proc Technol* **19**: 325-337 (2013).
6. Blasco J, Aleixos N, Gómez J and Moltó E, Citrus sorting by identification of the most common defects using multispectral computer vision. *J Food Eng* **83**: 384-393 (2007).
7. Mo C, Kim G, Kim MS, Lim J, Cho H, Barnaby JY, et al., Fluorescence hyperspectral imaging technique for foreign substance detection on fresh-cut lettuce. *J Sci Food Agric* **97**: 3985-3993 (2017).
8. Hu MH, Dong QL and Liu BL, Modelling postharvest quality of blueberry affected by biological variability using image and spectral data. *J Sci Food Agric* **96**: 3365-3373 (2016).
9. Lee H, Kim MS, Song YR, Oh CS, Lim HS, Lee WH, et al., Non-destructive evaluation of bacteria-infected watermelon seeds using visible/near-infrared hyperspectral imaging. *J Sci Food Agric* **97**: 1084-1092 (2017).
10. Dong C-w, Ye Y, Zhang J-q, Zhu H-k and Liu F, Detection of thrips defect on green-peel citrus using hyperspectral imaging technology combining pca and b-spline lighting correction method. *J Integr Agric* **13**: 2229-2235 (2014).
11. Li J, Rao X and Ying Y, Detection of common defects on oranges using hyperspectral reflectance imaging. *Comput Electron Agric* **78**: 38-48 (2011).
12. Blasco J, Ortiz C, Sabater MD and Molto E, Early detection of fungi damage in citrus using nir spectroscopy, in *Environmental and Industrial Sensing*, Ed. SPIE, p 8 (2000).
13. Gómez-Sanchis J, Gómez-Chova L, Aleixos N, Camps-Valls G, Montesinos-Herrero C, Moltó E, et al., Hyperspectral system for early detection of rottenness caused by penicillium digitatum in mandarins. *J Food Eng* **89**: 80-86 (2008).
14. Gómez-Sanchis J, Martín-Guerrero JD, Soria-Olivas E, Martínez-Sober M, Magdalena-Benedito R and Blasco J, Detecting rottenness caused by penicillium genus fungi in citrus fruits using machine learning techniques. *Expert Syst Appl* **39**: 780-785 (2012).
15. Lorente D, Blasco J, Serrano AJ, Soria-Olivas E, Aleixos N and Gómez-Sanchis J, Comparison of roc feature selection method for the detection of decay in citrus fruit using hyperspectral images. *Food Bioproc Tech* **6**: 3613-3619 (2013).
16. Lorente D, Escandell-Montero P, Cubero S, Gómez-Sanchis J and Blasco J, Visible–nir reflectance spectroscopy and manifold learning methods applied to the detection of fungal infections on citrus fruit. *J Food Eng* **163**: 17-24 (2015).
17. Gómez-Sanchis J, Blasco J, Soria-Olivas E, Lorente D, Escandell-Montero P, Martínez-Martínez JM, et al., Hyperspectral lctf-based system for classification of decay in mandarins caused by penicillium digitatum and penicillium italicum using the most relevant bands and non-linear classifiers. *Postharvest Biol Technol* **82**: 76-86 (2013).
18. Gómez-Sanchis J, Lorente D, Soria-Olivas E, Aleixos N, Cubero S and Blasco J, Development of a hyperspectral computer vision system based on two liquid crystal tuneable filters for fruit inspection. Application to detect citrus fruits decay. *Food Bioprocess Technol* **7**: 1047–1056 (2014).
19. Balasundaram D, Burks TF, Bulanon DM, Schubert T and Lee WS, Spectral reflectance characteristics of citrus canker and other peel conditions of grapefruit. *Postharvest Biol Technol* **51**: 220-226 (2009).
20. Li J, Chen L, Huang W, Wang Q, Zhang B, Tian X, et al., Multispectral detection of skin defects of bi-colored peaches based on vis–nir hyperspectral imaging. *Postharvest Biol Technol* **112**: 121-133 (2016).
21. Barkai-Golan R, Novel approaches for enhancing host resistance, in *Postharvest diseases of fruits and vegetables*. Elsevier, Amsterdam, pp. 252-266 (2001).
22. Qin J, Burks TF, Zhao X, Niphadkar N and Ritenour MA, Development of a two-band spectral imaging system for real-time citrus canker detection. *J Food Eng* **108**: 87-93 (2012).
23. Li J, Rao X and Ying Y, Development of algorithms for detecting citrus canker based on hyperspectral reflectance imaging. *J Sci Food Agric* **92**: 125-134 (2012).

24. Lorente D, Aleixos N, Gómez-Sanchis J, Cubero S and Blasco J, Selection of optimal wavelength features for decay detection in citrus fruit using the roc curve and neural networks. *Food Bioproc Tech* **6**: 530-541 (2013).
25. Baranowski P, Mazurek W, Wozniak J and Majewska U, Detection of early bruises in apples using hyperspectral data and thermal imaging. *J Food Eng* **110**: 345-355 (2012).
26. Kaliramesh S, Chelladurai V, Jayas DS, Alagusundaram K, White NDG and Fields PG, Detection of infestation by callosobruchus maculatus in mung bean using near-infrared hyperspectral imaging. *J Stored Prod Res* **52**: 107-111 (2013).